

Journal of Biomedical Optics

BiomedicalOptics.SPIEDigitalLibrary.org

Descriptive parameters of the erythrocyte aggregation phenomenon using a laser transmission optical chip

Martín A. Toderi
Horacio V. Castellini
Bibiana D. Riquelme

SPIE.

Martín A. Toderi, Horacio V. Castellini, Bibiana D. Riquelme, "Descriptive parameters of the erythrocyte aggregation phenomenon using a laser transmission optical chip," *J. Biomed. Opt.* **22**(1), 017003 (2017), doi: 10.1117/1.JBO.22.1.017003.

Descriptive parameters of the erythrocyte aggregation phenomenon using a laser transmission optical chip

Martín A. Toderi,^{a,*} Horacio V. Castellini,^b and Bibiana D. Riquelme^{a,c}

^aÓptica Aplicada a la Biología, IFIR (CONICET-UNR), Rosario, Santa Fe, Argentina

^bFacultad de Ciencias Exactas Ingeniería y Agrimensura, Departamento de Física, UNR, Rosario, Santa Fe, Argentina

^cFacultad de Cs. Bioquímicas y Farmacéuticas, Área Física, UNR, Rosario, Santa Fe, Argentina

Abstract. The study of red blood cell (RBC) aggregation is of great interest because of its implications for human health. Altered RBC aggregation can lead to microcirculatory problems as in vascular pathologies, such as hypertension and diabetes, due to a decrease in the erythrocyte surface electric charge and an increase in the ligands present in plasma. The process of erythrocyte aggregation was studied in stasis situation (free shear stresses), using an optical chip based on the laser transmission technique. Kinetic curves of erythrocyte aggregation under different conditions were obtained, allowing evaluation and characterization of this process. Two main characteristics of blood that influence erythrocyte aggregation were analyzed: the erythrocyte surface anionic charge (EAC) after digestion with the enzyme trypsin and plasmatic protein concentration in suspension medium using plasma dissolutions in physiological saline with human albumin. A theoretical approach was evaluated to obtain aggregation and disaggregation ratios by syllectograms data fitting. Sensible parameters (Amp_{100} , $t_{1/2}$) regarding a reduced erythrocyte EAC were determined, and other parameters (AI, M-Index) resulted that are representative of a variation in the plasmatic protein content of the suspension medium. These results are very useful for further applications in biomedicine. © 2017 Society of Photo-Optical Instrumentation Engineers (SPIE) [DOI: [10.1117/1.JBO.22.1.017003](https://doi.org/10.1117/1.JBO.22.1.017003)]

Keywords: optical chip; laser transmission; syllectogram; erythrocyte aggregation; aggregation parameters.

Paper 160750R received Nov. 3, 2016; accepted for publication Jan. 4, 2017; published online Jan. 31, 2017.

1 Introduction

Phenomena associated with red blood cell (RBC) aggregation have been of interest for many years. Most studies involve various scientific areas, such as blood rheology and *in vivo* clinical medicine observations. Research carried out in recent years has focused on two areas: (a) mechanisms of aggregation and the role of cellular features in the formation of aggregates and (b) importance of *in vivo* RBC aggregation and its role as a determinant of blood flow and vascular resistance.^{1,2} Consequently, the development of techniques and equipment, which allow evaluation and characterization of this process in a fast and efficient way, is of great importance.

Erythrocytes tend to form aggregates that initially consist of face-to-face linear structures resembling a stack of coins, which are generally called “rouleaux.”³ The characteristics of RBC aggregation can be analyzed by different methods and techniques,^{4,5} with light transmission being one of the most commonly used.^{6,7} In previous studies, a device based on this phenomenon was developed in our laboratory in order to carry out experiments regarding RBC aggregation at different sample volumes.⁸ The curve of light transmission versus time after the aggregation process has begun is called syllectogram.⁹ Image processing is also an important tool to study these phenomena. Recently, Kaliviotis et al.¹⁰ analyzed local aggregation of RBCs in microchannels by bright-field microscopy imaging, also

assessing the velocity of the erythrocytes and hematocrit. Commercial equipment presents different configurations and requires different sample volumes. Additionally, mathematical techniques to analyze the syllectogram have to be applied, resulting in different parameters representative of the phenomenon. These parameters should reflect different aspects involved in RBC aggregation phenomena.

The erythrocyte membrane consists of three basic components: a lipid bilayer, transmembrane proteins, and a cytoskeletal network.^{11,12} The presence of sialic acid residues in glycoproteins results in negative EAC, which keeps RBCs dispersed by electrostatic repulsion forces. Furthermore, these negative charges favor the uniform distribution of proteins of the glycocalyx on the surface of the membrane, (keeping an equidistance between them). Hence, a lower sialic acid content involves a disturbance in the rheological properties of the membrane and produces greater and more disordered aggregation.^{2,13} In addition, the presence of fibrinogen in plasma is determinant to RBCs' aggregation due to its role as a bonding protein, being mainly responsible for the formation of clumps.¹⁴⁻¹⁶

1.1 Red Blood Cell Aggregation in Pathologies

The characterization of the erythrocyte aggregation phenomenon is important to analyze possible alterations in microcirculation, observed in certain vascular diseases, such as hypertension and diabetes,^{17,18} as well as hematologic alterations,¹⁹ and in

*Address all correspondence to: Martín A. Toderi, E-mail: martintoderi@gmail.com

conditions produced *in vitro* by the action of different agents, such as phytochemicals, biomaterials, drugs, and anesthetics components.^{20,21} In addition, recent work has demonstrated its importance for the understanding of vascular disturbances in obese patients²² and after removing tourniquets.²³ In vascular diseases such as diabetes and hypertension, the shape of rouleaux is altered, producing large globular aggregates that can lead to a blockage in microcirculation.^{14,24} These obstructions reduce the disintegrating forces, resulting in an incremental increase in the size of the aggregates, consequently disturbing the mentioned flow and causing a feedback situation, which leads to an escalation of blood viscosity.²⁵ It is, therefore, of great interest to have accessible methods to quantify the characteristics of the RBC aggregation phenomenon in order to assess more accurately hemorheological alterations in pathologies of this kind. Current devices which serve this purpose are of considerable dimensions and are not suitable for day-to-day clinical use. In addition, a large volume of blood sample is generally required (between 1 and 100 mL),^{10,26-29} which can make this kind of practice more complex. Mobile and washable parts also represent a drawback, therefore, a simple and compact device is needed.

1.2 Red Blood Cell Interaction as a Potential

A suspension of RBCs in physiological medium is a stable or metastable state that can be outlined as a result of the action of two types of opposing forces: the cohesive forces that tend to attract the cells and the repulsive forces that tend to separate them. In such a system, at the solid-liquid interface, there is a contact phase characterized by the presence of ionized molecules in which the effects are modulated by Brownian motion. Surface phenomena involved in the stability of the

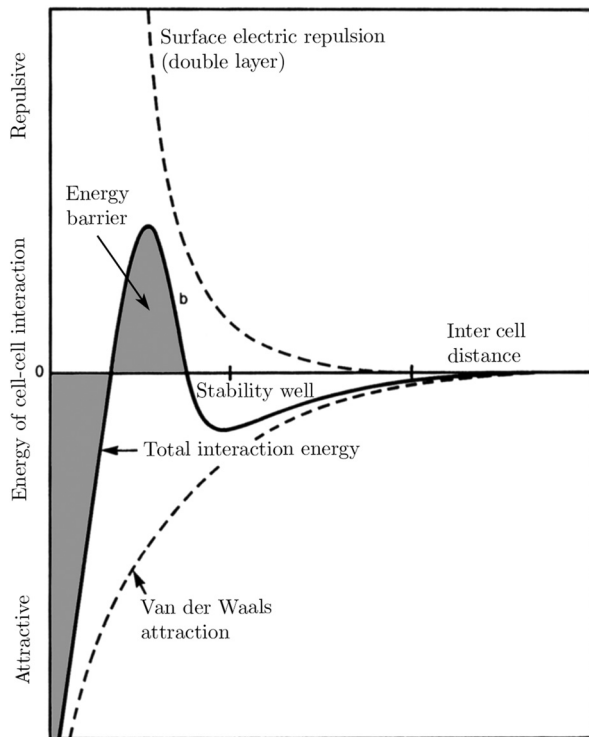


Fig. 1 Electrical energy curve for erythrocyte aggregates in an aqueous medium.

suspensions are particularly important in the formation of rouleaux. Attractive Van der Waals forces and purely electrostatic repulsive forces can be modeled by a resulting energy potential, introduced by Stern in combination with DLVO theory for aqueous dispersions.³⁰⁻³² Figure 1 shows the two interactions and the total electric potential, which presents a minimum that characterizes the stability distance (well) between cells. This stability well traps RBCs long enough time so that the ligands can establish the protein bridge (fibrinogen) that generates RBC aggregation.

1.3 Theoretical Background

Kaliviotis and Yianneskis³³ proposed that the formation of aggregates is similar to the sedimentation phenomenon. A competition of two phenomena is assumed: on the one hand, aggregation, and on the other, spontaneous disaggregation, the latter being proportional to the number of RBCs. From the Smoluchowski equation, the following equation is obtained:³³

$$\frac{dN}{dt} = -\frac{1}{2}AN^2 + \frac{1}{2}DN_0, \tag{1}$$

where A is the aggregation ratio and D is the disaggregation ratio. $N(t) = \sum_{i=1}^{\infty} n_i(t)$ is the total number of aggregates, with $n_i(t)$ the quantity of rouleaux of i RBCs of length. $N_0 = \sum_{i=1}^{\infty} in_i(t)$ is the total number of RBCs, defined as $N_0 = \sum_{i=2}^{\infty} in_i(t)$, which is supposed to remain constant during the measurement. Integrating Eq. (1) with null initial conditions, that is, supposing that all of the RBCs are initially disaggregated, the following equation for the total number of aggregates as a function of time is obtained:

$$N(t) = N_0 \sqrt{\frac{D}{A}} \tan h(N_0 \sqrt{AD}t). \tag{2}$$

In this equation, when $t \rightarrow 0$, $N(t) \approx N_0^2 D^2 t$ results, thus, the initial slope is proportional to the disaggregation ratio (D).

1.4 Aggregation Parameters

Analyzing the syllectograms, as described by Shin et al.,³⁴ different indices can be established to characterize the aggregation kinetics.^{4,7,26} The parameters calculated after data normalization are outlined in Fig. 2, and are defined as follows:

- Amplitude (Amp_t): The light intensity amplitude at a given time t , indicating the extent of RBC aggregates.

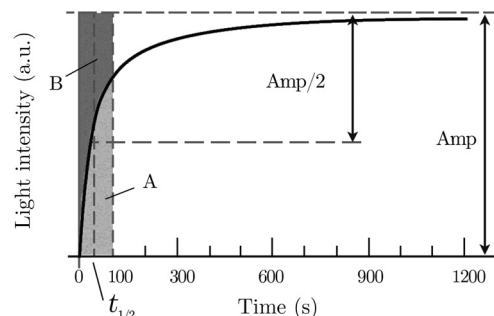


Fig. 2 Diagram of aggregation parameters in the syllectogram.

- Half time ($t_{1/2}$): The time required to reach the light intensity $Amp/2$, indicating the characteristic time constant for the average level of aggregation at a given time.
- M-Index_{*t*}: The area below the syllectogram in a period of time, indicating the degree of aggregate accumulation during that time. For example, in Fig. 2, at $t = 100$ s, M-Index = A.
- Aggregation Index (AI_{*t*}): The ratio of the area below the syllectogram (A) and the total area (A + B) in a certain period of time, indicating the normalized amount of accumulated RBC aggregates. For example, in Fig. 2, at $t = 100$ s, $AI_{100} = A/(A + B)$.

2 Materials and Methods

Samples of peripheral blood from healthy donors were used under bioethical criteria established by the Bioethics Committee of the Facultad de Ciencias Bioquímicas y Farmacéuticas, Universidad Nacional de Rosario (res. No. 1072/14 on December 19, 2014). All donors gave informed written consent to participate. Blood was drawn by venipuncture, anticoagulated with EDTA and stored at 4°C until use. RBCs were obtained from whole blood by centrifugation at 500 g (PWL Parawall Model 12T) for 5 min at 25°C. Plasma was separated and stored at 4°C for later use. Buffy coat was discarded and RBCs were washed three times with physiological saline (PS) (Laboratorio de Especialidades Medicinales, Rosario, Argentina, lot: 1072, exp. Sep 17). All procedures were performed according to the “New Guidelines for Hemorheological Laboratory Techniques.”³⁵

2.1 In Vitro Alterations of Aggregation Factors

Different hematocrits: In order to assess hematocrit dependence on the parameters, suspensions of RBCs in plasma starting at 30% and increasing by 5% until 50% is reached were prepared.

RBCs with decreased EAC: The study of cellular factors that influence erythrocyte aggregation was modeled by digestion of glycocalyx with solutions of trypsin, a peptidase enzyme that breaks the protein bonds. RBCs were incubated for 20 min at 37°C with a solution of trypsin (Sigma Lot. 70H0439) in PS at 1, 2 and 2.5 mg/mL concentrations.¹³

Alteration of plasma protein content: Studies of alterations in suspending medium were performed by reducing the concentration of the fibrinogen, responsible for the bonding between erythrocytes. A solution of human albumin (20%, Lab. de

Hemoderivados, UNC, Argentina, lot: AH1525/50-20, exp. July 29, 2018) at 2% in PS (PSA) was then prepared. Dilutions of plasma in PSA at 0%, 25%, 50%, 75%, were used to vary the plasma protein content, mainly that of fibrinogen. Albumin was used due to its weak effect on RBCs aggregation and the fact that it prevents erythrocyte crenation by the glass effect.^{36,37}

2.2 Optical Chip Aggregometer

The device was designed for small volume samples (15 μ L) and was based on the laser transmission phenomenon. The device is a simplified variant of a previously developed equipment,³⁴ which is based on laser transmission to assess erythrocyte aggregation. Our device has a disposable optical chip, which holds a small volume blood samples (15 μ L) and consists of a 1-mm thick glass slide with a 1.8-mm thick piece of double-sided plastic tape, as shown in Fig. 3(a). The measurement device sets the sample on a horizontal plane, as shown in Fig. 3(b). A diode laser beam (Melles-Griot, 670 nm, 5 mW) goes through the sample and a photomultiplier (Rudolph Technologies) records the transmitted laser intensity. Amp parameters were calculated for 100 and 750 s, $t_{1/2}$, and M-Index and AI were considered for the total time of the measurement (1500 s).

Figure 3(a) shows a scheme of the chip, which was placed on the support plate, between the photomultiplier and mirror, matching the beam path with one of the test chambers, as shown in Fig. 3(b). Blood was stirred gently for 1 min with a micropipette to disaggregate the cells that were in stasis without producing violent clashes of the cells against the walls of the tube for every measurement; no inversion of the sample was done, in order to keep the RBC integrity. Microscope imaging was used to verify effective disaggregation by this stirring method in all tested samples. Injection of the sample also acts as a mechanism of disaggregation, because the diameter of the pipette tip is very small. The experiment was recorded for 25 min right after injecting the previously stirred blood in the test chamber (the time window between disaggregation and injection is less than 2 s), and transmitted laser intensity and time elapsed were obtained. Later, these data were subjected to custom-made software processing. Syllectograms (graphics of light intensity versus time) were obtained, from which aggregation parameters were calculated. Previous studies on different volume samples showed that 15 μ L was the optimal volume for our set up.⁸ In this work, experiments were conducted with a fixed chamber geometry, a cylinder holding 15 μ L of blood sample. The obtained results were analyzed and modeled to

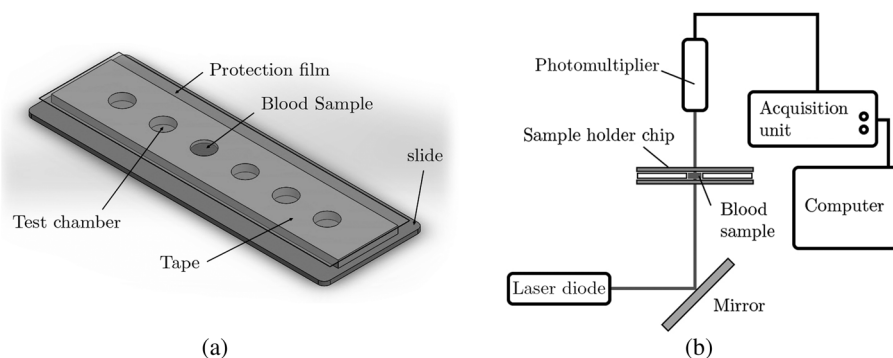


Fig. 3 Simplified diagrams of the measuring device: (a) optical chip and (b) setup.

determine and characterize the proposed parameters more accurately.

3 Results

3.1 Hematocrit Dependence

Studies varying hematocrit in the physiological range (30% to 50%) shows that Amp_{100} decreases, and $t_{1/2}$ increases as the hematocrit rises [Figs. 4(a) and 4(b)], showing a sensitivity to the quantity of cells in the test chamber. However, Amp_{750} , M-Index, and AI are invariant to hematocrit, not showing significant variations within the analyzed hematocrit range, as shown in Figs. 4(c)–4(e).

3.2 Alterations on the Red Blood Cell Surface Anionic Charge

The reduction of erythrocyte EAC produces an increase in the rate of laser transmission associated with increased RBCs' aggregation during the process. For these studies, eight measurements of each sample (control, treated with trypsin 1 mg/mL, 2 mg/mL and 2.5 mg/mL) were performed within 24 h of blood sample preparation. Figure 5 shows the microscopic image of the samples, evidencing more globular and disordered rouleaux as the concentration of trypsin used for the incubation increases. A total of 32 measurements were analyzed and processed, aggregation parameters were calculated in each case, and then an average and standard deviation of the indices

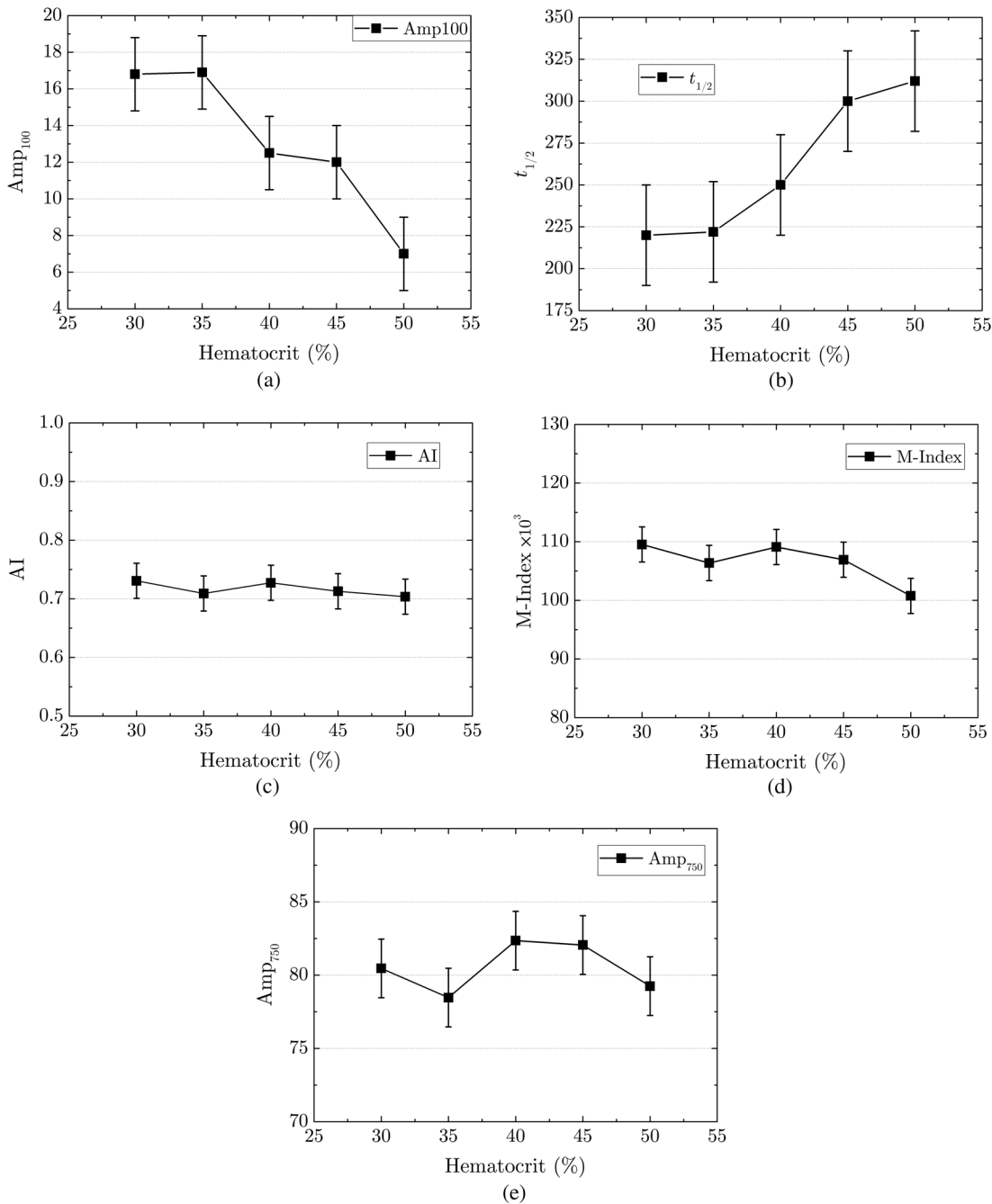


Fig. 4 Hematocrit dependence of parameters: (a) Amp_{100} ; (b) $t_{1/2}$; (c) AI; (d) Amp_{750} , and (e) M-Index. Mean values were obtained from four measurements of each hematocrit.

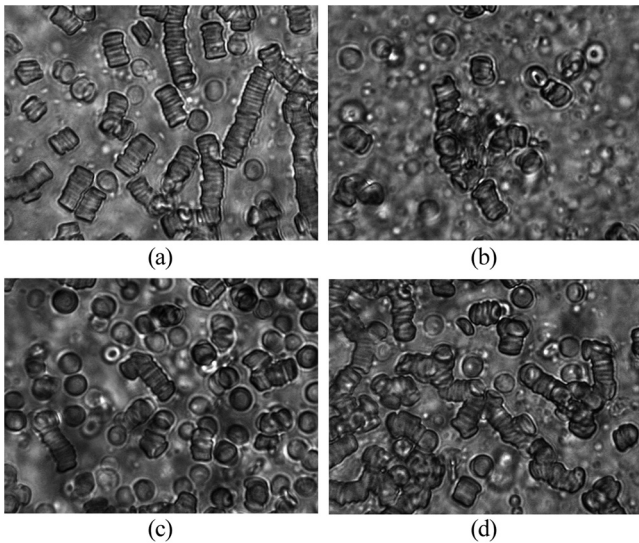


Fig. 5 Digital images obtained with an optical microscope with an objective 40x of RBCs from control and treated with trypsin samples: (a) control; (b) 1 mg/mL; (c) 2 mg/mL, and (d) 2.5 mg/mL.

for each type of sample was obtained, as shown in Table 1. A linear fitting of the data was also performed in the first seconds of the process (between 125 and 300 s), to assess the behavior by the value of the slope obtained by linear fit.

Figure 6 simultaneously shows fitted normalized syllectograms after 200 s for control and different *in vitro* treatments with various concentrations of trypsin, responsible for reductions of EAC. The extrapolation to 0 s in this figure was automatically depicted by the software. At this stage, the hematocrit was kept constant at 40%. The curve corresponding to the treatment with the highest concentration of trypsin is above the other curves and has a faster growth.

3.3 Alterations in Plasma Protein Content

In vitro reduction of protein ligands in plasma was performed by dilution of plasma with PSA, in order to test the sensibility of the aggregation parameters, regarding a variation in the bonding factors of erythrocytes (e.g., fibrinogen). In the images of Fig. 7, it can be seen how much scarcer aggregates are as plasma becomes more diluted. In samples with 0% plasma, crenated RBCs are found due to the glass effect. Additionally, RBCs lose the capacity to aggregate because of the absence of ligands, consequently, phenomena of RBCs' sedimentation play an

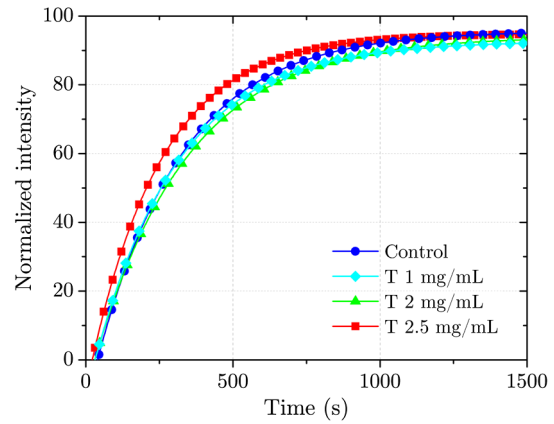


Fig. 6 Syllectogram of tests with different concentrations of trypsin from suspensions of RBCs in plasma at 40%.

important role in the generation of the syllectogram at this stage. Table 2 shows the calculated parameters for these tests.

Figure 8 shows the fitting of the normalized syllectogram after 200 s for these tests, evidencing the consequences of alterations in the presence of ligand protein. Likewise, here the extrapolation to 0 s was automatically depicted by the software. The results corresponding to the medium with the low concentration of plasma proteins (25% and 0% of plasma) are located below the other curves and present a more linear behavior.

3.4 Data Fitting Parameters

Parameters A and D were determined by computational fitting of the syllectograms and by using Eq. (2) and are presented in Table 3. In Fig. 9(a), a crossover is observed after 200 s, where there is a slope change possibly due to a preponderance of RBCs' sedimentation over the aggregation. Data fitting was considered for the second part of the syllectogram, as shown in Fig. 9(b).

4 Discussion

The most important differences observed in samples of reduced EAC are exhibited by the RBCs treated with the highest concentration of trypsin (2.5 mg/mL). In this case, the aggregation phenomenon takes place at a faster rate, leading to greater aggregation in the first minutes and a lower $t_{1/2}$. On the other hand, total aggregation does not present significant variations. RBCs with reduced surface anionic charge have a greater tendency to form globular aggregates,¹⁴ implying higher rates of aggregation

Table 1 Aggregation parameters obtained from eight measurements for each RBC suspension (control, trypsin 1, 2, and 2.5 mg/mL). Results are presented as average \pm standard deviation.

| Samples | Amp ₁₀₀ | Amp ₇₅₀ | $t_{1/2}$ | AI ₁₅₀₀ | M-Index ₁₅₀₀ $\times 10^3$ | Slope of linear fit between 125 and 300 s |
|-------------------|--------------------|--------------------|--------------|--------------------|---------------------------------------|---|
| Control | 12.1 \pm 1.1 | 82.0 \pm 2.1 | 284 \pm 31 | 0.716 \pm 0.025 | 107.4 \pm 3.6 | 0.242 \pm 0.003 |
| Trypsin 1 mg/mL | 14.6 \pm 2.5 | 83.0 \pm 2.7 | 278 \pm 28 | 0.717 \pm 0.017 | 107.6 \pm 2.5 | 0.211 \pm 0.003 |
| Trypsin 2 mg/mL | 15.5 \pm 2.5 | 84.7 \pm 2.2 | 250 \pm 15 | 0.725 \pm 0.021 | 108.7 \pm 3.0 | 0.199 \pm 0.003 |
| Trypsin 2.5 mg/mL | 19.0 \pm 1.8 | 86.4 \pm 2.4 | 226 \pm 18 | 0.738 \pm 0.032 | 110.8 \pm 4.7 | 0.218 \pm 0.003 |

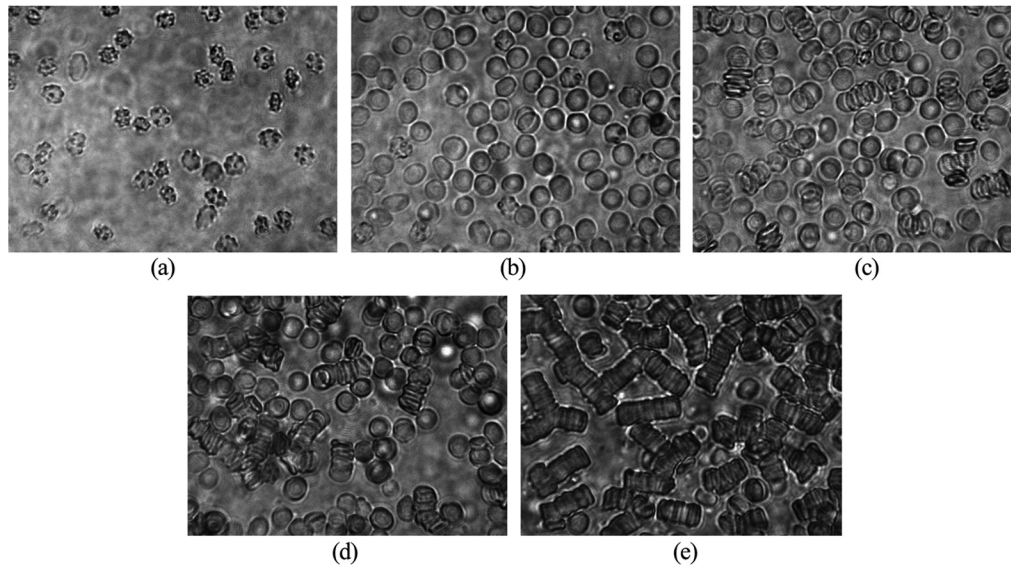


Fig. 7 Digital images obtained with an optical microscope with 40× objective of RBCs suspended in diluted plasma: (a) 0% plasma, (b) 25% plasma, (c) 50% plasma, (d) 75% plasma, and (e) control 100% plasma.

Table 2 Aggregation parameters obtained from eight measurements for each RBCs suspension (control and plasma with PSA in concentrations of 0%, 25%, 50%, and 75%). The results are presented as average ± standard deviation.

| Samples | Amp ₁₀₀ | Amp ₇₅₀ | <i>t</i> _{1/2} | AI ₁₅₀₀ | M-Index ₁₅₀₀ × 10 ³ | Slope 170:300 s |
|--------------|--------------------|--------------------|-------------------------|--------------------|---|-----------------|
| Plasma 100 % | 12.8 ± 0.8 | 89.0 ± 1.6 | 267 ± 16 | 0.90 ± 0.01 | 115.5 ± 1.1 | 0.224 ± 0.003 |
| Plasma 75 % | 11.3 ± 5.4 | 85.3 ± 1.8 | 283 ± 2 | 0.72 ± 0.01 | 107.5 ± 0.3 | 0.220 ± 0.005 |
| Plasma 50 % | 13.2 ± 1.4 | 80.9 ± 4.5 | 334 ± 18 | 0.68 ± 0.03 | 104.0 ± 2.6 | 0.194 ± 0.006 |
| Plasma 25 % | 8.6 ± 0.2 | 66.5 ± 2.2 | 429 ± 8 | 0.56 ± 0.03 | 84.6 ± 4.2 | 0.170 ± 0.008 |
| Plasma 0 % | 7.6 ± 1.1 | 73.7 ± 3.7 | 443 ± 8 | 0.62 ± 0.02 | 93.5 ± 2.2 | 0.179 ± 0.008 |

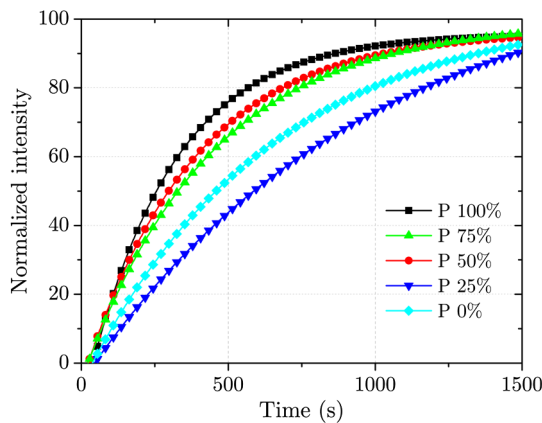


Fig. 8 Sylllectogram of RBCs at 40% hematocrit with different dilutions of plasma with PSA.

characterized by high *t*_{1/2} and Amp₁₀₀ values. The results correlate with the ones obtained by Shin et al.,³⁴ where dextran (70 kD) was used to modulate a higher aggregation rate. Also, our results, which were obtained for a time lapse of 25 min taking into account the aggregation-sedimentation

Table 3 Values of A and D calculated by computational fitting for different samples: control, RBCs with reduced EAC by trypsin (2 mg/mL), and altered plasma protein content.

| Samples | Aggregation ratio (A) × 10 ⁻⁴ | Disaggregation ratio (D) × 10 ⁻⁴ |
|-------------------|--|---|
| Control | 22 ± 6 | 19 ± 5 |
| Trypsin (2 mg/mL) | 26 ± 6 | 23 ± 5 |
| Plasma 75 % | 22 ± 6 | 21 ± 5 |
| Plasma 50 % | 21 ± 6 | 19 ± 5 |
| Plasma 25 % | 13 ± 6 | 13 ± 5 |
| Plasma 0 % | 25 ± 6 | 14 ± 5 |

process, are consistent with those measured in similar samples by laser backscattering technique in the first 40 s of the process.^{13,38}

Dilution of plasma with PSA has a reducing effect on aggregation. This is due to a decrease in the concentration of plasma

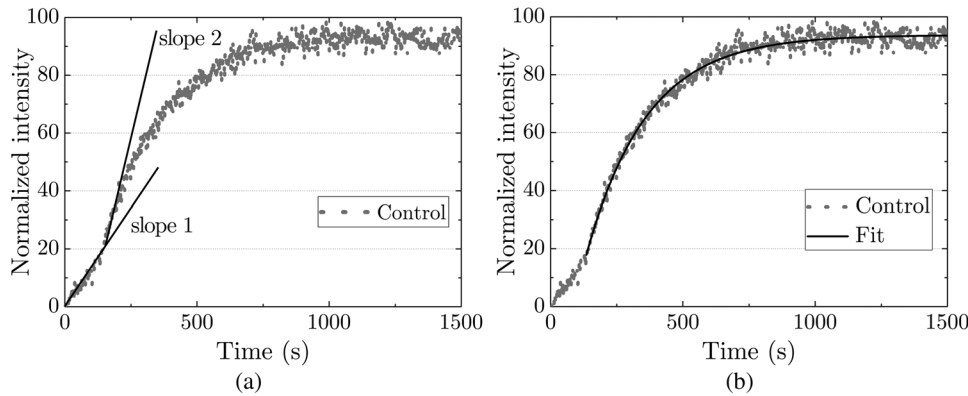


Fig. 9 Sylllectograms of control RBC at 40% hematocrit: (a) slope crossover during aggregation phenomenon and (b) computational fit neglecting “slope 1” behavior.

proteins, especially fibrinogen, which induces bonding among erythrocytes. Our results suggest that $t_{1/2}$ increases as plasma dilution diminishes and AI and the M-Index, representing the cumulative degree of aggregation, have lower values than the control sample.

Amp₁₀₀ and $t_{1/2}$ proved to be sensitive to hematocrit variation while AI, M-Index, and Amp₇₅₀ parameters do not show significant discrepancy within the hematocrit physiological range.

A and D rates, calculated by data fitting, are higher in the case of RBCs with altered EAC, indicating a greater tendency to rouleaux formation, and are lower when the presence of fibrinogen in the plasma is reduced, denoting a lower aggregation.

5 Conclusion

Characterizing parameters used in the present work would allow the detection of alterations similar to those found in blood samples of patients with vascular pathologies, parasitosis,³⁹ and other microcirculatory disorders, as well as alterations in plasma protein content commonly caused by anesthetics.²¹ In this respect, this device is meant to be simple. The fact that it only uses a 15- μ L volume sample and the development of a disposable optical chip reinforces the concept of a device suitable for clinical use. Firsthand information obtained in a matter of minutes is of great help in a medical environment. This study would contribute to the assessment of possible alterations in RBC aggregation, relating them with their causes.

Disclosures

The authors report that no relevant conflicts of interest originated from this study.

Acknowledgments

Authors thank Dr. Mabel D’Arrigo director of the Clinical Analytical Chemistry Laboratory of the FCByF (UNR) for the collaboration and direction in the preparation of biological samples and the English Department of FCByF (UNR) for their assistance in the language correction of this manuscript. First author thanks the Consejo Interuniversitario Nacional and the Universidad Nacional de Rosario for their financial support to these studies.

References

- O. Baskurt, B. Neu, and H. J. Meiselman, *Red Blood Cell Aggregation*, CRC Press, Boca Raton (2011).
- R. Skalak and C. Zhu, “Rheological aspects of red blood cell aggregation,” *Biorheology* **27**, 309–325 (1990).
- S. Chien and L. A. Sung, “Physicochemical basis and clinical implications of red cell aggregation,” *Clin. Hemorheol.* **7**, 71–91 (1987).
- O. K. Baskurt, H. Meiselman, and E. Kayar, “Measurement of red blood cell aggregation in “a plate–plate” shearing system by analysis of light transmission,” *Clin. Hemorheol. Microcirc.* **19**(4), 307–314 (1998).
- A. Priezhev et al., “Aggregation and disaggregation of erythrocytes in whole blood: study by backscattering technique,” *J. Biomed. Opt.* **4**(1), 76–84 (1999).
- J. Nam et al., “Comparison of light-transmission and -backscattering methods in the measurement of red blood cell aggregation,” *J. Biomed. Opt.* **15**(2), 027003 (2010).
- M. Uyklu et al., “Wavelength selection in measuring red blood cell aggregation based on light transmittance,” *J. Biomed. Opt.* **16**(11), 117006 (2011).
- M. A. Toderi, H. V. Castellini, and B. D. Riquelme, “Simplified variant of an optical chip to evaluate aggregation of red blood cells,” *Proc. SPIE* **9531**, 95313X (2015).
- R. Brinkman, W. G. Zijlstra, and N. J. Jansonius, “Quantitative evaluation of the rate of rouleaux formation of erythrocytes by measuring light reflection (“sylllectometry”),” *Proc. Koninklijke Nederlandse Akad. Wetenschappen. C. Biol. Med. Sci.* **66**, 236–248 (1966).
- E. Kaliviotis et al., “Quantifying local characteristics of velocity, aggregation and hematocrit of human erythrocytes in a microchannel flow,” *Clin. Hemorheol. Microcirc.* **63**(2), 123–148 (2016).
- B. Alberts, D. Bray, and J. Lewis, *Molecular Biology of the Cell*, 4th ed., Garland Science, New York (2002).
- E. A. Evans and R. Skalak, *Mechanics and Thermodynamics of Biomembranes*, CRC Press, Boca Raton, Florida (1980).
- G. Del Balzo et al., “Study of trypsin effect on erythrocyte surface charge using a laser backscattering technique,” *Anales AFA* **22**(1), 88–91 (2010).
- H. Schmid-Schönbein et al., “Pathological red cell aggregation (clump aggregation). Molecular and electrochemical factors,” *Bibl. Anat.* **16**(2), 484–9 (1977).
- M. Aleman et al., “Fibrinogen and red blood cells in venous thrombosis,” *Thrombo. Res.* **133**(1), S38–S40 (2014).
- C. Wagner, P. Steffen, and S. Svetina, “Aggregation of red blood cells: from rouleaux to clot formation,” *C.R. Phys.* **14**(6), 459–469 (2013).
- P. Foresto et al., “Evaluación de alteraciones hemorreológicas,” *Medicina (B. Aires)*, **65**, 121–125 (2005).
- G. Mazarevica, T. Freivalds, and A. Jurka, “Properties of erythrocyte light refraction in diabetic patients,” *J. Biomed. Opt.* **7**(2), 244–247 (2002).
- R. J. Rasia, “Quantitative evaluation of erythrocyte viscoelastic properties from diffractometric data: applications to hereditary spherocytosis,

- thalassaemia and hemoglobinopathy," *Clin. Hemorheol.* **15**(2), 177–189 (1995).
20. V. Danieli et al., "Tratamiento de eritrocitos humanos con copolímeros sintéticos: optimización del tiempo de incubación," *Acta Bioquím. Clín. Latinoam.* **43**(1), 43–48 (2009).
 21. A. Alet et al., "Hemorheological in vitro action of propofol on erythrocytes from healthy donors and diabetic patients," *Clin. Hemorheol. Microcirc.* **64**(2), 157–165 (2016).
 22. W. Maciej et al., "Sex-dependent differences in rheological properties and the relation of blood viscosity to erythrocyte aggregation indices among morbidly obese patients," *Clin. Hemorheol. Microcirc.* **44**(4), 259–67 (2010).
 23. P. Connes et al., "Sampling time after tourniquet removal affects erythrocyte deformability and aggregation measurements," *Clin. Hemorheol. Microcirc.* **41**(1), 9–15 (2009).
 24. M. Delannoy et al., "Influence of hypertension and type 2 diabetes mellitus on erythrocyte aggregation using image digital analysis," *Ser. Biomech.* **29**(1), 5–10 (2015).
 25. S. Shin et al., "Shear-dependent aggregation characteristics of red blood cells in a pressure driven microfluidic channel," *Clin. Hemorheol. Microcirc.* **34**, 353–362 (2006).
 26. M. Hardeman, J. Dobbe, and C. Ince, "The laser-assisted optical rotational cell analyzer (LORCA) as red blood cell aggregometer," *Clin. Hemorheol. Microcirc.* **25**(1), 1–11 (2001).
 27. M. Hardeman et al., "Laser-assisted optical rotational cell analyser (L.O.R.C.A.); I. A new instrument for measurement of various structural hemorheological parameters," *Clin. Hemorheol. Microcirc.* **14**(4), 605–618 (1994).
 28. L. Plá et al., "Cold-agglutinin hemolytic diseases, a rheo-optical study," *Clin. Hemorheol. Microcirc.* **38**(2), 83–91 (2008).
 29. F. T. Yu et al., "Ultrasonic parametric imaging of erythrocyte aggregation using the structure factor size estimator," *Biorheology* **46**(4), 343–363 (2009).
 30. S. Glasstone, *Tratado de Química Física*, Aguilar, Madrid (1964).
 31. E. Moelwyn-Hughes, *Physical Chemistry*, Pergamum Press, Oxford (1961).
 32. D. Gramhame, "The electrical double layer and the theory of electrocapillarity," *Chem. Rev.* **41**(3), 441–501 (1947).
 33. E. Kaliviotis and M. Yianneskis, "Blood viscosity modelling: influence of aggregate network dynamics under transient conditions," *Biorheology* **48**(2), 127–47 (2011).
 34. S. Shin, Y. Yang, and J.-S. Suh, "Measurement of erythrocyte aggregation in a microchip stirring system by light transmission," *Clin. Hemorheol. Microcirc.* **41**(3), 197–207 (2009).
 35. O. K. Baskurt et al., "New guidelines for hemorheological laboratory techniques," *Clin. Hemorheol. Microcirc.* **42**, 75–97 (2009).
 36. L. Eriksson, "On the shape of human red blood cells interacting with flat artificial surfaces—the 'glass effect'," *Biochim. Biophys. Acta* **1036**, 193–201 (1990).
 37. D. Aldana, J. Brailsford, and B. Bull, "Red cell membrane crenation: a macromodel of the echinocyte," *J. Theor. Biol.* **140**, 185–192 (1989).
 38. M. Delannoy et al., "Arterial hypertension modeled by in vitro treatment of red blood cells," *Ser. Biomech.* **27**(1–2), 87–92 (2012).
 39. P. Ponce de León et al., "In vitro alterations of erythrocyte aggregation by action of *Trichinella spiralis* newborn larvae," *Clin. Hemorheol. Microcirc.* 1–10 (2016).

Martín A. Toderi is a doctoral student at the Institute of Physics Rosario (CONICET-UNR) in the group of Optics Applied to Biology under the direction of Professor Bibiana D. Riquelme, in Rosario, Argentina. He holds of a doctoral scholarship granted by CONICET. He is an assistant professor at the FCBYF. He received his degree of Licenciado en Física in 2015 at the FCEIA from the UNR. His current research interests include biophysics, hemorheology, and laser optics.

Biographies for the other authors are not available.